Segregation of global and local motion processing in primate middle temporal visual area

Richard T. Born & Roger B. H. Tootell

Department of Neurobiology, Harvard Medical School,
220 Longwood Avenue, Boston, Massachusetts 02115, USA

THE early stages of primate visual processing appear to be divided up into several component parts so that, for example, colour, form and motion are analysed by anatomically distinct streams[1-3]. We have found that further subspecialization occurs within the motion processing stream. Neurons representing two different kinds of information about visual motion are segregated in columnar fashion within the middle temporal area of the owl monkey. These columns can be distinguished by labelling with 2-deoxyglucose in response to large-field random-dot patterns. Neurons in lightly labelled interbands have receptive fields with antagonistic surrounds: the response to a centrally placed moving stimulus is suppressed by motion in the surround. Neurons in more densely labelled bands have surrounds that reinforce the centre response so that they integrate motion cues over large areas of the visual field. Interband cells carry information about local motion contrast that may be used to detect motion boundaries or to indicate retinal slip during visual tracking. Band cells encode information about global motion that might be useful for orienting the animal in its environment.

Our first hint that the middle temporal visual area (MT) had a modular organization came from studies with 2-deoxyglucose in which a large-field random-dot stimulus moving coherently at systematically varied directions, speeds and binocular disparities failed to produce uniform isotope uptake within this area (Fig. 1; ref. 4). We consistently obtained columnar patterns that were often band-like and regular but were occasionally more patchy, as in Fig. 1. We refer to the columns of high 2-deoxyglucose uptake as 'bands' and the intervening low-uptake regions as 'interbands'. This topography corresponds only roughly to the previously described pattern of cytochrome oxidase staining in owl monkey area MT[5]. We have chosen to use 2-deoxyglucose as our reference because it more directly reflects the functional properties of neurons and the cytochrome oxidase patterns are not consistently present in different primate species, whereas 2-deoxyglucose patterns are similar and consistent in both New and Old World monkeys.

The findings using 2-deoxyglucose prompted us to study the properties of single units in area MT with respect to their position in the band-interband architecture. In nine tangential and nine perpendicular microelectrode penetrations through area MT in anaesthetized, paralysed Aotus monkeys we recorded from 245 single units. The recording technique and stimulus generation have been described[6]. After qualitative characterization of the best direction, speed and binocular disparity for each cell, the extent and nature of centre-surround interactions were measured using two sets of stimuli: (1) circular windows of varying diameter that contained random dots moving coherently in the cell's preferred direction (area summation test), and (2) a centre bar moving in the cell's preferred direction while the direction of motion of a surround patch of random dots was varied (surround direction test).

We found two major classes of neurons in area MT (Fig. 2e). The first class responded more vigorously as the stimulus size was increased (Fig. 2a). The excitatory effect of increased patch size often extended well beyond the borders of the receptive field as mapped with a single bar, thus indicating the presence of a surround whose action reinforced the centre's directional response. Small bars were usually ineffective stimuli for these cells (Fig. 2b, bar); they responded best in the surround direction test when the large surround field of random dots moved in the same direction as that preferred by the centre (Fig. 2b). The second major class failed to respond to large fields of coherently moving stimuli, indicating the presence of a surround that was antagonistic to the centre response (Fig. 2c). The suppressive surround was sometimes direction-selective, so that motion in the surround at the same direction and speed as the centre motion inhibited the response, whereas surround motion in the opposite direction actually enhanced the response over that to the centre stimulus alone (Fig. 2d). In other cells, any motion in the surround was inhibitory regardless of its direction (Fig. 4b, top, right-hand graph).

During the nine tangential penetrations, we consistently found that neurons with similar centre-surround interactions were clustered (Fig. 3). In three of these penetrations we used 2-deoxyglucose to label the band-interband architecture after completing the single unit recording. When the electrode track was reconstructed and superimposed on an autoradiograph of the 2-deoxyglucose-labelled tissue, the cells whose receptive fields had antagonistic surrounds were located in the light interbands, and the cells whose receptive fields had reinforcing surrounds were located predominantly in the dark bands (Fig. 3a). By staining the sections for cytochrome oxidase[7] or cresyl violet or both, we determined the laminar position of each unit recorded (Fig. 3b); this allowed us to tell whether changes in unit properties were due to horizontal or laminar position.

The columnar nature of the band-interband architecture was confirmed by electrode penetrations perpendicular to the cortical surface. In these penetrations we always found that one receptive field type dominated, with virtually all the exceptions in the upper parts of layers 4 and 6 (Fig. 4). We determined the laminar position of 118 neurons during the nine perpendicular penetrations. Of these, only 19 neurons (16%) were discordant with their column type (almost always a neuron lacking an antagonistic surround, in an interband), and 16 of these 19
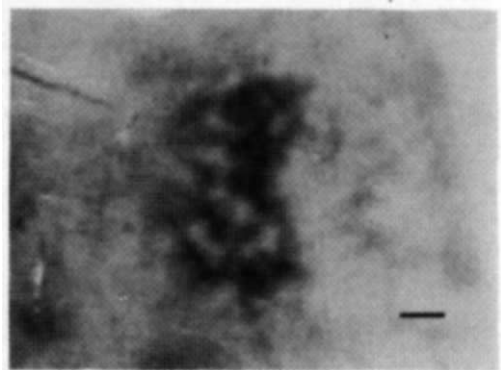

FIG. 1 Band-interband architecture of area MT as shown by the 2-deoxyglucose method. An anaesthetized, paralysed Aotus monkey was injected intravenously with ^{14}C-labelled-deoxyglucose while it binocularly viewed a large field (60° in diameter) of random dots that were systematically drifted in all directions and at a variety of speeds. The 2-deoxyglucose protocol and subsequent histological processing have been described[22]. Scale bar, 1 mm.
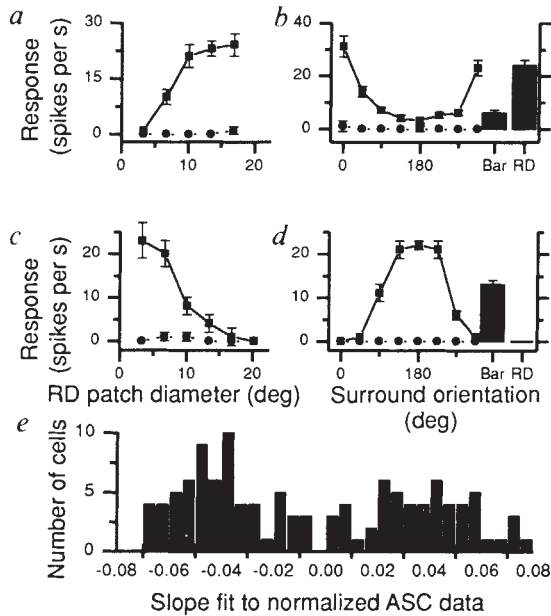
FIG. 2 Two major cell classes in area MT. a–d, Stimulus-response curves from one band cell (a, b) and one interband cell (c, d). a and c, Area summation curves showing each cell's response to patches of coherently moving random dots. Increasing values on the abscissa indicate progressively larger circular areas of the visual field stimulated with random dots (dot density was constant). The smallest patch size was always well within the borders of the cell's receptive field as mapped by a single bar. b and d, Surround direction tuning curves in which the centre of each cell's receptive field was stimulated with an optimally moving bar while the direction of motion of a surrounding field of random dots was varied. Zero degrees means that the surround dots moved in the same direction as the centre bar, and 180 degrees means that the surround dots moved in the opposite direction. The centre-surround interactions shown in the line plots should be compared with the adjacent column plots which show the cell's response to a centre bar moving on a stationary field of random dots (Bar) and a large field ($>20°$) of random dots moving in the cell's preferred direction while the centre bar was stationary (RD). Note that in d, the presence of surround dots moving in a direction opposite to the best direction for the centre bar increased the response over that to the bar alone. The filled squares connected by solid lines indicate the response while the stimulus was on and moving, and the filled circles connected by dotted lines indicate the cell's level of spontaneous activity just prior to each stimulus presentation. Each point is the average of five trials. Error bars are +/− one standard deviation. e, Histogram of the slopes of regression lines fit to the normalized area summation curves for 118 unslected single units. It is extremely unlikely that this sample was drawn from a single normally distributed population ($P < 0.00001$, Shapiro-Wilk W test for normality). Quantile analysis gave a sigmoidal curve with the inflection point at zero, indicating a bimodal distribution.

(84%) were in layer 4 or the top of layer 6. In layers 2 and 3, only one of 48 (2%) units failed to match its column type.

Neurons whose receptive fields manifest centre-surround interactions for moving stimuli have been described previously in primate area MT[8-11], in cat superior colliculus[12] and in pigeon optic tectum[13,14]. In primate area MT there is a tendency for antagonistic surround inhibition to distribute laminarly, being more prevalent in the supra- and infragranular layers and tending to avoid layer 4 (refs 10, 11). Our results in the owl monkey

agree with these results, and in addition we find that cells in the uppermost part of layer six also often lack antagonistic surrounds, even in the interbands. Both of these thin layers receive inputs from striate cortex[15].

In addition to a laminar organization, we found a horizontal clustering of centre-surround interactions, which was constant with respect to cortical depth. The overall architecture is thus predominantly columnar with thin gaps in the striate recipient layers. This situation is analogous to the columnar orientation

FIG. 3 Reconstruction of a tangential penetration through area MT. a, Electrode track superimposed on the 2-deoxyglucose-labelled band–interband pattern. Each single unit is represented by a dot whose brightness indicates the degree of surround inhibition. The degree of surround inhibition was measured as the slope of the regression line fit to the normalized area summation curve, as in Fig. 2e. If the slope was greater than or equal to zero, the cell was classified as non-surround inhibited (white); if the slope was less than zero but greater than −0.03, the cell was deemed weakly surround inhibited (grey); and if the slope was less than or equal to −0.03 (indicating at least a halving of the cell's best response), the cell was called strongly surround-inhibited (black). b, The same penetration at an expanded scale showing the laminar position of each unit (top). The solid dark bars represent the result of a densitometric scan along the electrode track taken from the 2-deoxyglucose image in a. Circles show the degree of surround inhibition (classified as described in a) for each unit. Note that the cluster of three interband cells that lack surround inhibition (just after 3,000 µm) was located in the uppermost part of layer 6, which receives inputs from striate cortex[15]. Abbreviations: A, anterior; P, posterior; D, dorsal; V, ventral; STS, superior temporal sulcus; SI, surround inhibition.
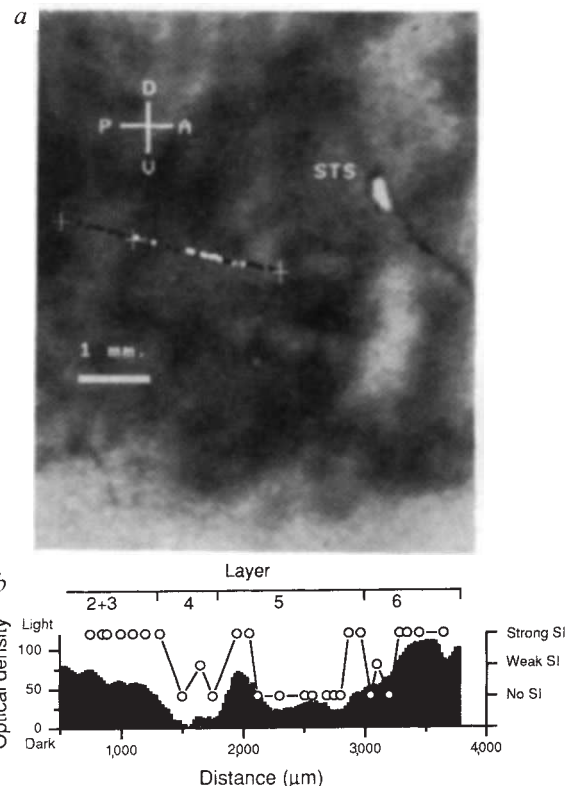
FIG. 4 Electrode track reconstructions of two vertical penetrations through area MT showing the columnar nature of the band-interband architecture. a, Cresyl violet/cytochrome oxidase histology of a presumptive band penetration with single units coded for the strength of surround inhibition as in Fig. 2. Both lesions are visible in this section: one near the middle of layers 2/3 and the other between layers 4 and 5. Immediately to the left are area summation curves of six single units recorded at the positions indicated. The stimulus protocol used to generate these curves was identical to that for Fig. 1a and c. b, Corresponding data for a presumptive interband penetration superimposed on the cresyl violet histology. Two of the three lesions are clearly visible in this section: one between layers 5 and 6 and another, larger lesion in the white matter. A third lesion, faintly visible in this section near the top of layer 4, is more obvious in the adjacent section (not shown). For this penetration, surround direction tuning curves are also shown because some of the surround-inhibited units gave poor responses even to the smallest diameter random dot fields (for example, topmost unit graphed.).
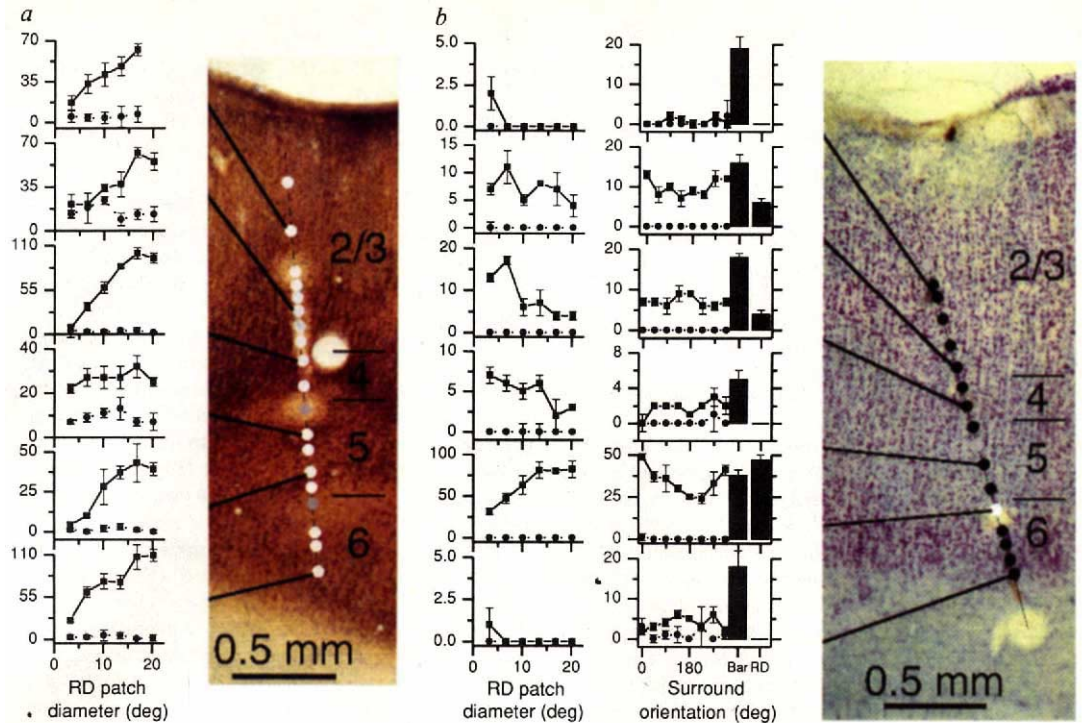
The presence of a strong non-direction-selective surround inhibition can be seen by comparing the cell's response to a centre bar alone (Bar) with the responses when there is surround motion. Any motion in the surround, regardless of direction, was inhibitory.

architecture in macaque striate cortex where parvocellular geniculate input layers can lack orientation selectivity[16]. This does not mean that MT neurons are strictly dichotomous with respect to surround antagonism. Indeed, the histogram of area summation curve slopes (Fig. 2e) shows cells with intermediate degrees of surround antagonism, consistent with the fact that band–interband boundaries are not perfectly sharp (Fig. 3b).

We believe that this columnar organization indicates that parallel processing is taking place within the motion pathway. The neurons with antagonistic surrounds in area MT seem to be calculating local motion contrast, analogous to the calculation of local intensity contrast performed by retinal ganglion cells[17]. This kind of information could be useful for perceptual popout[18], as a signal from an object boundary moving with respect to the background[9], due either to true object motion or to observer motion when the object and background are at different depths (motion parallax). Another possibility is that local motion contrast cells whose receptive fields are near the fovea provide, during visual tracking, an image velocity signal, which behavioral experiments have indicated is a necessary input to the smooth pursuit system[19].

Cells within the bands differ from interband cells in that they sum motion cues over relatively large regions of the visual field. This type of operation is necessary for the calculation of global motion properties, such as optic flow, which, combined with vestibular and proprioceptive information, help the animal orient to and navigate within its environment. It is also clear that cells with such large excitatory integrating receptive fields could provide the inhibitory surrounds for interband cells, although we have no direct evidence that band cells serve this role.

This anatomical segregation within MT may be the precursor to a more complete parcellation of these two broad categories of information about visual motion. The principal projection area of MT in the macaque, area MST, consists of two separate representations of the visual field, MSTd and MSTl, whose receptive field properties resemble those of band and interband cells, respectively[20]. It has been recently reported that a dorsal subdivision of area FST (the owl monkey homologue of MST) receives inputs from an array of cell clusters within area MT (ref. 21). It would be interesting to know if these parallel projections map on to the band–interband architecture. □

1. Livingstone, M. S. & Hubel, D. H. Science 240, 740–749 (1988).
2. DeYoe, E. A. & Van Essen, D. C. Trends Neurosci. 11, 219–226 (1988).
3. Maunsell, J. H. R. & Newsome, W. T. A. Rev. Neurosci. 10, 363–440 (1987).
4. Tootell, R. B. H. & Born, R. T. Invest. ophthalmol. visual Sci. 31, 238 (1990).
5. Tootell, R. B. H., Hamilton, S. L. & Silverman, M. S. J. Neurosci. 5, 2786–2800 (1985).
6. Born, R. T. & Tootell, R. B. H. Proc. natn. Acad. Sci. U.s.A. 88, 7066–7070 (1991).
7. Wong-Riley, M. T. T. Brain Res. 171, 11–28 (1979).
8. Baker, J. F., Petersen, S. E., Newsome, W. T. & Allman, J. M. J. Neurophysiol. 45, 397–416 (1981).
9. Allman, J., Miezin, F. & McGuinness, E. Perception 14, 105–126 (1985).
10. Tanaka, K., Hikosaka, K. & Saito, H. J. Neurosci. 6, 134–144 (1986).
11. Lagae, L., Gulyas, B., Raiguel, S. & Orban, G. A. Brain Res. 496, 361–367 (1989).
12. Sterling, P. & Wickelgren, B. G. J. Neurophysiol. 32, 1–15 (1969).
13. Frost, B. J., Scilley, P. L. & Wong, S. C. P. Expl Brain Res. 43, 173–185 (1981).
14. Frost, B. J. & Nakayama, K. Science 220, 744–745 (1983).
15. Rockland, K. S. Vis. Neurosci. 3, 155–170 (1989).
16. Hubel, D. H. & Wiesel, T. N. J. Physiol., Lond. 195, 215–243 (1968).
17. Kuffler, S. W. J. Neurophysiol. 16, 37–68 (1953).
18. Treisman, A. Sci. Am. 255, 106–115 (1986).
19. Krauzlis, R. J. & Lisberger, S. G. Neural Comp. 1, 116–122 (1989).
20. Wurtz, R. H., Duffy, C. J. & Roy, J. P. Cold Spring Harb Symp. quant. Biol. LV, 45 (1990).
21. Kaas, J. H. & Morel, A. E. Invest. ophthalmol. vis. Sic. 33, 1219 (1992).
22. Tootell, R. B. H., Hamilton, S. L., Silverman, M. S. & Switkes, E. J. Neurosci. 8, 1500–1530 (1988).